PROCEEDINGS OF SCIENCE

ONLINE ICRC 2021
THE ASTROPARTICLE PHYSICS CONFERENCE
Berlin | Germany
37th International Cosmic Ray Conference
12–23 July 2021

KM3NeT Core Collapse Supernovae observation program in standalone and multi-messenger modes

Alexis Coleiro,[a] **Damien Dornic,**[b] **Vladimir Kulikovskiy,**[c,*] **Massimiliano Lincetto,**[b] **Marta Colomer Molla**[a,d] **and Godefroy Vannoye**[b,e] **on behalf of the KM3NeT Collaboration**
(a complete list of authors can be found at the end of the proceedings)

[a] *Université de Paris, CNRS, AstroParticule et Cosmologie, F-75013, Paris, France*
[b] *Aix Marseille University, CNRS/IN2P3 CPPM, Marseille, France*
[c] *IINFN Sezione di Genova, Via Dodecaneso 33, Genova, 16146, Italy*
[d] *Instituto de Física Corpuscular (CSIC-Universitat de València) c/ Catedrático José Beltrán, 2 E-46980 Paterna, Valencia, Spain*
[e] *Ecole Normale Supérieure de Lyon,, 15 parvis René Descartes BP 7000 69342 Lyon Cedex 07 FRANCE*
E-mail: vkulikovskiy@km3net.de

The KM3NeT research infrastructure in the Mediterranean is a multi-purpose cubic-kilometre neutrino observatory consisting of two detectors optimised to study cosmic and atmospheric neutrinos between GeV to PeV energies. Additionally, KM3NeT multi-photomultiplier optical modules allow the detection of nearby MeV interaction products by selecting nanosecond coincidences within the photomultipliers of the same module. The distribution of the number of photomultipliers forming a coincidence (multiplicity) for the whole supernova emission is used as a proxy of the average neutrino energy. Using an optimised coincidence selection the KM3NeT detectors will be sensitive to supernovae in our Galaxy and beyond. A high number of detected events from a core collapse supernovae explosion is expected in KM3NeT thanks to its large effective volume. The measurement of the neutrino light curve properties, such as the light curve start time and the presence of the standing accretion shock instability oscillations is possible with such statistics. Sub-millisecond time synchronisation between KM3NeT detectors allows joint observation. Such a scheme can be also a viable solution to synchronise the KM3NeT telescopes with other detectors aiming to observe neutrino emission from core collapse supernovae through the SNEWS network.

37th International Cosmic Ray Conference (ICRC 2021)
July 12th – 23rd, 2021
Online – Berlin, Germany

*Presenter

© Copyright owned by the author(s) under the terms of the Creative Commons Attribution-NonCommercial-NoDerivatives 4.0 International License (CC BY-NC-ND 4.0).

1. Detection of CCSN neutrinos in KM3NeT

The KM3NeT neutrino detectors, ARCA and ORCA, are under construction in the Mediterranean Sea [1]. Composed primarily of three-dimensional optical module arrays, their granularity is optimised for the detection of atmospheric GeV neutrinos (ORCA) to study the neutrino oscillations and cosmic TeV–PeV neutrinos (ARCA) to perform astronomical searches.

Each KM3NeT optical module is composed of thirty-one 3 inch photomultipliers (PMTs). Although for 10 MeV scale neutrino energies the light detection by multiple KM3NeT optical modules is rarely possible, several PMTs of the same module are typically hit simultaneously. An increased rate of such events with high number of hit photomultipliers (so-called multiplicity) on a second time scale is a signature of the supernova neutrino emission as it is studied in this work. The optical modules are installed in groups of 18 on flexible lines moored at the bottom of the sea at depths of about 3500 m (ARCA) and 2500 m (ORCA). The detectors installation is modular and currently ARCA and ORCA are continuously taking data with 6 lines each (ARCA6 & ORCA6).

In our work [2], the supernova detection sensitivities are evaluated using the fluxes and neutrino light curves predicted by 3D simulations. The considered fluxes correspond to the cases of two CCSNe from progenitors with respective masses of $11M_\odot$ and $27M_\odot$ [3, 4], and a so-called *failed* supernova with a progenitor of $40M_\odot$ [5] collapsing into a black hole. A fourth CCSN progenitor of $20M_\odot$ [3, 4], with enhanced accretion shock oscillations, is used in the light curve studies.

The following interaction channels of low-energy neutrinos in water producing CCSN signal in KM3NeT are considered:

- inverse beta decay (IBD) of electron anti-neutrinos on free protons ($\bar{\nu}_e + p \rightarrow e^+ + n$): 88–93% of neutrinos are detected through this channel, favoured by its relatively large cross section and efficient transfer of the incident neutrino energy to the outgoing positron;
- elastic scattering on electrons ($\nu + e^- \rightarrow \nu + e^-$): $3 - 5\%$ of the events, all neutrino flavours;
- interactions with oxygen nuclei ($\nu_e + {}^{16}\mathrm{O} \rightarrow e^- + {}^{16}\mathrm{F}$, $\bar{\nu}_e + {}^{16}\mathrm{O} \rightarrow e^+ + {}^{16}\mathrm{N}$): 2–8% of the events, depending on the progenitor;

1.1 Optical background

The background for this analysis is composed of three main components, as described below.

- Uncorrelated single photoelectron background originated from PMT dark rates and single-photon bioluminescence emission. For a 10 ns coincidence time window, these are negligible for multiplicity values above two. Bioluminescence can, however, impact the overall instantaneous number of active PMTs in the detector, as the signals from the PMTs which are above the high rate veto threshold are suppressed.
- Radioactive decays, dominating at low multiplicities, with a rate of 500 Hz for a multiplicity of two, decreasing roughly by one order of magnitude for every step in multiplicity.
- Cherenkov light from atmospheric muons, relevant for multiplicity values above 5 and dominating at multiplicities ≥ 8.

The background from atmospheric muons can be reduced by exploiting the correlated coincidences on multiple DOMs. As a first step to reduce this background and spurious PMT pulses (mainly afterpulses) coincidences on the same or on different DOMs are grouped with a time window of 1 μs for the ORCA detector and 3 μs for the ARCA detector. The KM3NeT trigger algorithms are designed to identify a minimum number of causally connected hits within extended cylindrical sections or localised spherical sections of the instrumented volume [1]. The data from the triggered events are used to define a veto on all the DOMs that have detected at least one triggered hit to further suppress the muon background. The effectiveness of the approach is verified on data taken with the previously operated ARCA2 and ORCA4 detectors. The μs-scale average duration of a muon veto multiplied by a muon trigger rate of ~ 10 Hz per building block results in a dead time fraction below 0.1%, which is negligible.

The efficiency of the background rejection is evaluated for one ARCA and one ORCA building block with Monte Carlo simulations. ARCA reaches a 65% rejection efficiency for multiplicity values above seven. In the same range, the denser geometry of the ORCA detector allows for the identification and suppression of more than 95% of the background. The difference is due to the fact that lower energy muons are not triggered in ARCA as efficiently as in ORCA. The impact of the filtering strategy on the signal is negligible, since the low energy CCSN neutrino interactions do not significantly contribute to the trigger rate.

2. Detection sensitivity

The sensitivity of KM3NeT to a CCSN neutrino burst is evaluated considering the number of signal and background events in a 500 ms time window. The length of the time window is chosen to cover the majority of the detectable neutrino emission, occurring in the accretion phase. In order to be compared with the signal simulation, the measured background rates are corrected for the measured average PMT detection efficiency. Then, the efficiency of the muon background rejection estimated in the ARCA and ORCA building block simulations is applied to the corrected rates to obtain the event rate of the background as a function of the multiplicity. In Figure 1 (left), the number of expected events for a single KM3NeT building block of 2070 DOMs is reported. The estimated backgrounds in ARCA and ORCA are compared with the simulated signal for the $11M_\odot$, $27M_\odot$ and $40M_\odot$ CCSN progenitors. From hereon, the computations account for the respective size of the complete KM3NeT detectors: two building blocks for ARCA and one for ORCA.

The sensitivity of a Poisson counting experiment to a given signal hypothesis can be defined as the expected median significance of its observation. In the large sample limit, the sensitivity, expressed in terms of Gauss standard deviations, can be approximated by the formula [7]:

$$Z = \sqrt{2\left((n_s + n_b)\,\ln\left(1 + \frac{n_s}{n_b}\right) - n_s\right)}, \tag{1}$$

where the expectation values for the number of signal (n_s) and background events (n_b) are used.

Considering the number of signal events as a function of the distance to the source, $n_s(d) = n_s(d_0)(d_0/d)^2$, with $d_0 = 10$ kpc, the $5\,\sigma$ discovery distance is evaluated as a function of the minimum and maximum multiplicities. The optimal sensitivity is achieved across the 7–10(12) multiplicity ranges for ARCA and in the (7)8–10(12) multiplicity ranges for ORCA, the parentheses

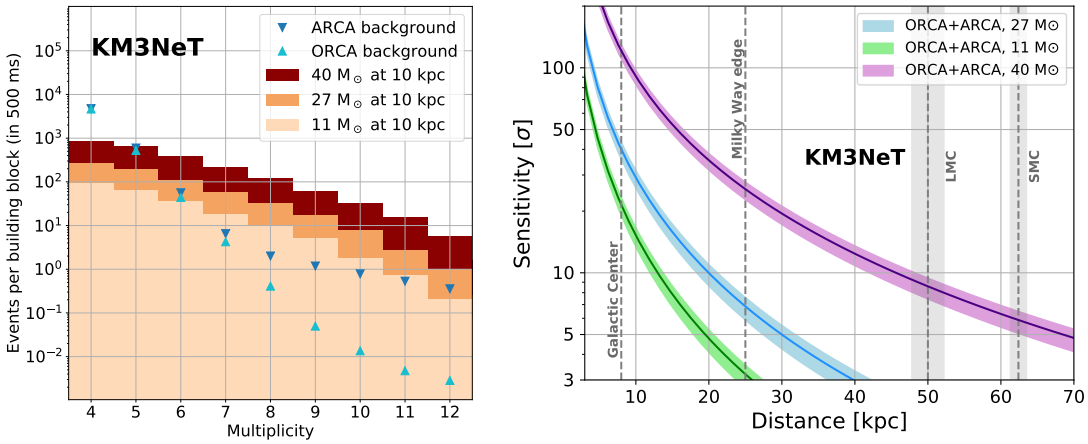

Figure 1: Left: expected number of events in a KM3NeT building block as a function of the multiplicity. The background is shown with markers in light blue for ORCA and dark blue for ARCA. The signal is represented with coloured bars in orange shades for the different models: light for $11M_\odot$, intermediate for $27M_\odot$, dark for $40M_\odot$. Right: KM3NeT detection sensitivity as a function of the distance to the CCSN for the three progenitors considered: $11M_\odot$ (green), $27M_\odot$ (blue) and $40M_\odot$ (purple). The error bars include the systematic uncertainties.

indicating that the same sensitivity is reached for both cuts. The final multiplicity range 7–11 is chosen by maximising the overall number of events and excluding the last multiplicity bin (12) where the background estimation is not reliable due to statistical fluctuations.

The sensitivity estimation includes the uncertainties on the determination of the neutrino interaction cross-sections ($< 1\%$), detection efficiency due to the water absorption variation (1%), PMT quantum efficiency variation ($\pm 10\%$) and fluctuating number of active PMTs (3%). The finite simulated volume has a negligible impact ($< 1\%$). The uncertainty of +15% affecting the filter efficiency underestimation is coming from the comparison of data with muons simulation.

Considering Z in (1) as a function of the distance, $Z(d)$, the KM3NeT combined sensitivity is obtained by using a weighted linear combination of the ORCA and ARCA sensitivities:

$$Z_{\mathrm{KM3NeT}}(d) = \frac{\sum_{\alpha\in\{\mathrm{ARCA,ORCA}\}} w_\alpha Z_\alpha(d)}{\sqrt{\sum_{\alpha\in\{\mathrm{ARCA,ORCA}\}} w_\alpha^2}}, \tag{2}$$

where the weight is defined as the sensitivity at a reference distance , $w_\alpha = Z_\alpha(d = 10\,\mathrm{kpc})$.

Taking into account the expected distribution of CCSNe as a function of the distance to the Earth [8], in the most conservative scenario considered in this work ($11M_\odot$), more than 95% of the Galactic core-collapse supernovae can be observed by the KM3NeT detectors.

2.1 Estimation of the neutrino spectrum parameters

The neutrino energy spectrum can be described in a simplified form as a quasi thermal distribution, which depends on the neutrino energy, E, and the time, t, relative to the core bounce [9]:

$$\frac{d\Phi}{dE\,dt}(E,t) = \frac{L(t)}{4\pi d^2}\frac{E^\alpha}{\Gamma(1+\alpha)}\left(\frac{1+\alpha}{\tilde{E}}\right)^{1+\alpha} e^{\frac{-E(1+\alpha)}{\tilde{E}}}, \tag{3}$$

where $\tilde{E}$ is the mean neutrino energy, L is the neutrino luminosity, d is the distance to the source, and α is the spectral shape parameter. The sensitivity to the averaged in time neutrino spectral parameters is estimated assuming perfect flavour equipartition.

The simulated data from ARCA and ORCA are combined in a 500 ms search window. The neutrino spectrum is characterised by three parameters: $\tilde{E}$, α, and the signal scale, Λ. The signal scale depends on the total energy released and the distance to the source. It is defined with respect to the benchmark values, $L_{\bar{\nu}_e,0} = 4 \cdot 10^{52}$ erg and $d_0 = 10$ kpc, as:

$$\Lambda = \frac{L_{\bar{\nu}_e}}{L_{\bar{\nu}_e,0}} \left(\frac{d_0}{d}\right)^2 . \tag{4}$$

The ability to constrain the parameters describing the neutrino energy spectrum is evaluated using a chi-square method on a multiplicity distribution of the detected events. Three different assumptions on the range of the α and Λ parameters are considered: they are known *a priori* (fixed), they are known in a constrained range given by $\alpha_{\text{true}} \pm 10\%$, $\Lambda_{\text{true}} \pm 10\%$, and α is a free parameter in the range of $2 - 4$,. The results are the following: the mean neutrino energy estimation has a 90% CL range of about ± 0.5 MeV (∼ 4%) when α and Λ are fixed and it stays below ± 1.5 MeV if these two parameters are known within a ±10% range. The sensitivity to the spectral parameters is lost if Λ and α are left free.

2.2 CCSN arrival time measurement

The arrival time of the burst, T_0, can be independently measured by KM3NeT. The first significant excess of selected events in the multiplicity range $7 - 11$ is used to define the time range of the fit and the starting point of the T_0 parameter. Then for the light curve analysis events with multiplicity ≥ 2 are considered. The background expectation value is subtracted and the obtained light curve is fitted with the function [10]:

$$R(t) = R_0 \Theta(t - T_0) \left(1 - e^{-\frac{t-T_0}{\tau}}\right), \tag{5}$$

where Θ is the step function, τ is the time constant of the light curve rise, and R_0 is the scale.

An average time resolution of 8 ms is achieved at the Galactic Centre (8 kpc) for the $20M_\odot$ progenitor, improving up to 3 ms for an equivalent source at 5 kpc. At 13 kpc, the uncertainty degrades down to 70 ms, with the fit failing in about 25% of the cases. At 14 kpc, the estimation becomes unreliable as the fraction of failed fits reaches 80%. For the $11M_\odot$ progenitor, a resolution of 7.5 ms is obtained at 5 kpc, degrading to about 70 ms at 8 kpc, with 35% of failed fits. The fraction of failed fits increases to about 85% at 9 kpc.

2.3 Detection of the standing accretion shock instability

A spectral analysis of the detected neutrino light curve is performed using a fast Fourier transform algorithm. From the model prediction, a time interval of [-150, 50] ms centred on the peak of the light curve is analysed. Two different strategies are adopted to estimate the probability of detecting the light curve oscillation expected in case of the standing accretion shock instability (SASI) [4, 11]. The first one (Method 1) is based on the measurement of the maximum of the power spectral density scanning over all frequency range and it is model-independent. Method 2

Table 1: Estimation of the sensitivity to SASI oscillations obtained combining ORCA and ARCA.

Progenitor	d [kpc]	Method 1	Method 2	Peak frequency (Hz)	Galactic coverage
27 $M_\odot$	3	$2.8 \pm 0.7\,\sigma$	$4.1 \pm 0.9\,\sigma$	80	3%
20 $M_\odot$	5	$3.2 \pm 0.7\,\sigma$	$4.5 \pm 0.9\,\sigma$	80	10%
40 $M_\odot$	8	$3.8 \pm 0.7\,\sigma$	$> 5\,\sigma$	140	35%

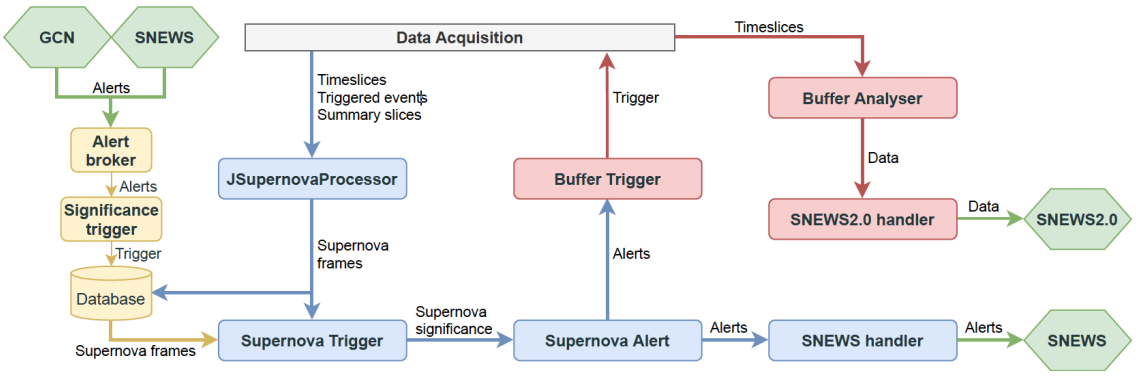

Figure 2: KM3NeT data acquisition scheme for the multi-messenger alert program.

is based on the integrated power in a designated frequency range, which is chosen to be ±20 Hz from the oscillation peak frequency known *a priori*. The significance is estimated by evaluating the average of each quantity on signal plus background simulation and calculating the p-value of the distribution of the same quantity estimated on the pure background. The p-value is expressed in sigmas (e.g. $3\sigma \approx 0.27\%$). The results are summarised in Table 1.

3. Multimessenger program

The experience of the multi-messenger community together with the enhanced capabilities of current and near-future neutrino detectors set a wider perspective for the coordinated detection of the next CCSN. A large multi-messenger follow-up campaign will be the key to achieve this goal. The SNEWS2.0 network [12], successor of the SNEWS [13], is also based on the detection of a coincident neutrino signal between experiments all around the world, and it will be enhanced with localisation, time-domain and spectrum studies. The combined false alert rate (FAR) of less than one per century is achieved by requiring a maximum FAR of one per 8 days in each single detector, and the coincidence between two or more detectors within 10 s.

An overview of the KM3NeT data acquisition system (DAQ) and real-time analysis framework is given in Figure 2. The KM3NeT detectors adopt an all-data-to-shore concept. The data filtering happens onshore. For the detection of high energy events the set of triggers searches for time-spacial correlations between DOMs with several photons detected. For the purpose of CCSN detection the DAQ records a separate stream containing all hits in coincidences with at least three other hits on PMTs within 90° axes and a time window of 15 ns.

This SN data stream is stored without preserving any coincidence information. In a dedicated application (supernova processor) a coincidence building algorithm is applied again on this data. The muons are vetoed using high energy event triggers and coincidences between DOMs as discussed in Section 1.1. Then, events with a PMT multiplicity of $7-11$ are selected as explained in Section 2 and they are referred to as SN events. While currently operating with small detectors, the multiplicity range is extended to 6–11 to compensate for the lower statistics of the background sample.

The probability of observing the given number of unique DOM detecting at least one SN event is calculated for the number of SN events and the total number of DOMs in both detectors. A low value of this probability may indicate the anomalies in the detector, i.e. excessive DOMs activity. A predefined probability threshold is required for a sample of SN events to validate the alert.

The detector efficiency is not constant in time since the number of active PMTs can be slightly reduced during periods of high bioluminescence activity. By performing simulations following the PMT rates in the previously collected data, the detector efficiency is parameterised as a function of the number of active PMTs. This is used to correct the signal expectation value according to the measured rates.

The combined sensitivity is estimated for 500 ms sliding windows with step of 100 ms using (2). The significance can be converted to the p-value and correspondingly to the false alarm rate considering sliding window rate of $(100\,\mathrm{ms})^{-1}$. The FAR threshold of 1/8 days is used to generate SNEWS alerts according the their requirements. Typically, the alert message is sent in less than 20 s from the arrival of the corresponding data on-shore. This makes KM3NeT one of the fastest alert sending experiments among the neutrino detectors participating in SNEWS, together with NOνA and HALO [12]. For the currently currently operating ARCA6 and ORCA6 detectors combined, KM3NeT is expected to be sensitive to CCSNe at distances below 11$\dot{\mathrm{k}}$pc for the $27\mathrm{M}_\odot$ progenitor. Events with an especially high significance, for which the equivalent FAR is below one per year, will be publicly advertised as a GCN circular.

An internal 10 min buffer in the onshore KM3NeT data filters is implemented to collect coincidences with multiplicity ≥ 2 within a 25 ns time window. This buffer can be dumped to storage upon an alert. The buffer is analysed to reconstruct the time profile of the signal filling time series of 1 ms with the number of coincidences. Here the time window for the coincidences is reduced to 5 ns to suppress the random background. The emission time, and the oscillation presence is then internally estimated according to the procedures defined in Sections 2.2, 2.3. The significance results together with the time series are planned to be distributed within SNEWS2.0. In particular, matching such light curve time series between several detectors may allow CCSN triangulaton on the sky in a model-independent way [14]. The internal dump of the buffer and subsequent analysis can be also triggered externally. The principal destination for this feature is the future SNEWS2.0 infrastructure. The data exchange will rely on the HOPSKOTCH publish-subscribe message system developed within the SCIMMA program [15].

The external triggers are analysed to derive the detection significance according to (2). In case of a low significance, an upper limit on the number of signal events can be set following Feldman and Cousins approach. A limit on the combined total energy and distance $L_\nu d^{-2}$ can also be derived assuming detailed ($27\mathrm{M}_\odot$ etc) or simplified quasi thermal distribution (3).

The GW event S200114f was identified on 14th January 2020 by the un-modelled LIGO-Virgo pipeline. This alert could could indicate the supernova emission in a region compatible with the

Galactic plane location. Two SN events were found in the ORCA4 data, while 1.4 were expected from background, after correcting for the estimated instrumentation efficiency. This excess is not significant, having a p-value of 0.4. The excluded distance corresponds to 6 kpc for $11M_{\odot}$, 11.5 kpc for $27M_{\odot}$ and 21 kpc for $40M_{\odot}$ which excludes one of the most promising progenitors, the Betelgeuse star which is close to the S200114f alert localisation.

4. Conclusions

The KM3NeT detectors are nowadays taking data with 6 lines on each of two sites. With this configuration KM3NeT is participating to the SNEWS network aiming for the detection of supernovae in our Galaxy or nearby. Once completed the KM3NeT detectors will have a joint 5σ sensitivity for more than 95% of the Galactic progenitors. High number of detected supernova neutrino interaction will allow time profile studies. Using this data a Galactic supernova position triangulation with other detectors is expected within the upcoming SNEWS2.0 network.

References

[1] S. Adrián-Martínez et al, J. Phys. G 43 (2016) 084001, 0.1088/0954-3899/43/8/084001.

[2] S. Aiello et al, Eur. Phys. J. C **81** (2021) 445 10.1140/epjc/s10052-021-09187-5.

[3] I. Tamborra et al, Phys. Rev. D **90** (2014) 4 045032 10.1103/PhysRevD.90.045032.

[4] I. Tamborra et al, Phys. Rev. Lett. **111** (2013) 12 121104 10.1103/PhysRevLett.111.121104.

[5] L. Walk et al, Phys. Rev. D **101** (2020) 12 123013 10.1103/PhysRevD.101.123013.

[6] A. Mirizzi et al, Riv. Nuovo Cim. **39** (2016) 1–2 10.1393/ncr/i2016-10120-8.

[7] G. Cowan et al, Eur. Phys. J. C **71** (2011) 1554 10.1140/epjc/s10052-011-1554-0.

[8] S. M. Adams et al, Astrophys. J. **778** (2013) 164 10.1088/0004-637X/778/2/164.

[9] M. T. Keil, PhD thesis, 2003, arXiv:astro-ph/0308228.

[10] R. Hansen, Phys. Rev. D **101** (2020) 12 123018 10.1103/PhysRevD.101.123018.

[11] T. Lund et al, Phys. Rev. D **82** (2010) 063007 10.1103/PhysRevD.82.063007.

[12] S. Al Kharusi et al, New J Phys., **23**.(2021) 031201 10.1088/1367-2630/abde33.

[13] P. Antonioli et al, New J. Phys., **6** (2004) 114 10.1088/1367-2630/6/1/114.

[14] A. Coleiro et al, Eur. Phys. J. C **80** (2020) 856, 10.1140/epjc/s10052-020-8407-7.

[15] A. L. Baxter et al, (2021), arXiv:2101.07779.

Full Author List: KM3NeT Collaboration

M. Ageron[1], S. Aiello[2], A. Albert[3,55], M. Alshamsi[4], S. Alves Garre[5], Z. Aly[1], A. Ambrosone[6,7], F. Ameli[8], M. Andre[9], G. Androulakis[10], M. Anghinolfi[11], M. Anguita[12], G. Anton[13], M. Ardid[14], S. Ardid[14], W. Assal[1], J. Aublin[4], C. Bagatelas[10], B. Baret[4], S. Basegmez du Pree[15], M. Bendahman[4,16], F. Benfenati[17,18], E. Berbee[15], A. M. van den Berg[19], V. Bertin[1], S. Beurthey[1], V. van Beveren[15], S. Biagi[20], M. Billault[1], M. Bissinger[13], M. Boettcher[21], M. Bou Cabo[22], J. Boumaaza[16], M. Bouta[23], C. Boutonnet[4], G. Bouvet[24], M. Bouwhuis[15], C. Bozza[25], H.Brânzaş[26], R. Bruijn[15,27], J. Brunner[1], R. Bruno[2], E. Buis[28], R. Buompane[6,29], J. Busto[1], B. Caiffi[11], L. Caillat[1], D. Calvo[5], S. Campion[30,8], A. Capone[30,8], H. Carduner[24], V. Carretero[5], P. Castaldi[17,31], S. Celli[30,8], R. Cereseto[11], M. Chabab[32], C. Champion[4], N. Chau[4], A. Chen[33], S. Cherubini[20,34], V. Chiarella[35], T. Chiarusi[17], M. Circella[36], R. Cocimano[20], J. A. B. Coelho[4], A. Coleiro[4], M. Colomer Molla[4,5], S. Colonges[4], R. Coniglione[20], A. Cosquer[1], P. Coyle[1], M. Cresta[11], A. Creusot[4], A. Cruz[37], G. Cuttone[20], A. D'Amico[15], R. Dallier[24], B. De Martino[1], M. De Palma[36,38], I. Di Palma[30,8], A. F. Díaz[12], D. Diego-Tortosa[14], C. Distefano[20], A. Domi[15,27], C. Donzaud[4], D. Dornic[1], M. Dörr[39], D. Drouhin[3,55], T. Eberl[13], A. Eddyamoui[16], T. van Eeden[15], D. van Eijk[15], I. El Bojaddaini[23], H. Eljarrari[16], D. Elsaesser[39], A. Enzenhöfer[1], V. Espinosa[14], P. Fermani[30,8], G. Ferrara[20,34], M. D. Filipović[40], F. Filippini[17,18], J. Fransen[15], L. A. Fusco[1], D. Gajanana[15], T. Gal[13], J. García Méndez[14], A. Garcia Soto[5], E. Garçon[1], F. Garufi[6,7], C. Gatius[15], N. Geißelbrecht[13], L. Gialanella[6,29], E. Giorgio[20], S. R. Gozzini[5], R. Gracia[15], K. Graf[13], G. Grella[41], D. Guderian[56], C. Guidi[11,42], B. Guillon[43], M. Gutiérrez[44], J. Haefner[13], S. Hallmann[13], H. Hamdaoui[16], H. van Haren[45], A. Heijboer[15], A. Hekalo[39], L. Hennig[13], S. Henry[1], J. J. Hernández-Rey[5], J. Hofestädt[13], F. Huang[1], W. Idrissi Ibnsalih[6,29], A. Ilioni[4], G. Illuminati[17,18,4], C. W. James[37], D. Janezashvili[46], P. Jansweijer[15], M. de Jong[15,47], P. de Jong[15,27], B. J. Jung[15], M. Kadler[39], P. Kalaczyński[48], O. Kalekin[13], U. F. Katz[13], F. Kayzel[15], P. Keller[1], N. R. Khan Chowdhury[5], G. Kistauri[46], F. van der Knaap[28], P. Kooijman[27,57], A. Kouchner[4,49], M. Kreter[21], V. Kulikovskiy[11], M. Labalme[43], P. Lagier[1], R. Lahmann[13], P. Lamare[1], M. Lamoureux[1,4], G. Larosa[20], C. Lastoria[1], J. Laurence[1], A. Lazo[5], R. Le Breton[4], E. Le Guirriec[1], S. Le Stum[1], G. Lehaut[43], O. Leonardi[20], F. Leone[20,34], E. Leonora[2], C. Lerouvillois[1], J. Lesrel[4], N. Lessing[13], G. Levi[17,18], M. Lincetto[1], M. Lindsey Clark[4], T. Lipreau[24], C. LLorens Alvarez[14], A. Lonardo[8], F. Longhitano[2], D. Lopez-Coto[44], N. Lumb[1], L. Maderer[4], J. Majumdar[15], J. Mańczak[5], A. Margiotta[17,18], A. Marinelli[6], A. Marini[1], C. Markou[10], L. Martin[24], J. A. Martínez-Mora[14], A. Martini[35], F. Marzaioli[6,29], S. Mastroianni[6], K. W. Melis[15], G. Miele[6,7], P. Migliozzi[6], E. Migneco[20], P. Mijakowski[48], L. S. Miranda[50], C. M. Mollo[6], M. Mongelli[36], A. Moussa[23], R. Muller[15], P. Musico[11], M. Musumeci[20], L. Nauta[15], S. Navas[44], C. A. Nicolau[8], B. Nkosi[33], B. Ó Fearraigh[15,27], M. O'Sullivan[37], A. Orlando[20], G. Ottonello[11], S. Ottonello[11], J. Palacios González[5], G. Papalashvili[46], R. Papaleo[20], C. Pastore[36], A. M. Păun[26], G.E. Păvălaş[26], G. Pellegrini[17], C. Pellegrino[18,58], M. Perrin-Terrin[1], V. Pestel[15], P. Piattelli[20], C. Pieterse[5], O. Pisanti[6,7], C. Poirè[14], V. Popa[26], T. Pradier[3], F. Pratolongo[11], I. Probst[13], G. Pühlhofer[51], S. Pulvirenti[20], G. Quéméner[43], N. Randazzo[2], A. Rapicavoli[34], S. Razzaque[50], D. Real[5], S. Reck[13], G. Riccobene[20], L. Rigalleau[24], A. Romanov[11,42], A. Rovelli[20], J. Royon[1], F. Salesa Greus[5], D. F. E. Samtleben[15,47], A. Sánchez Losa[36,5], M. Sanguineti[11,42], A. Santangelo[51], D. Santonocito[20], P. Sapienza[20], J. Schmelling[15], J. Schnabel[13], M. F. Schneider[13], J. Schumann[13], H. M. Schutte[21], J. Seneca[15], I. Sgura[36], R. Shanidze[46], A. Sharma[52], A. Sinopoulou[10], B. Spisso[41,6], M. Spurio[17,18], D. Stavropoulos[10], J. Steijger[15], S. M. Stellacci[41,6], M. Taiuti[11,42], F. Tatone[36], Y. Tayalati[16], E. Tenllado[44], D. Tézier[1], T. Thakore[5], S. Theraube[1], H. Thiersen[21], P. Timmer[15], S. Tingay[37], S. Tsagkli[10], V. Tsourapis[10], E. Tzamariudaki[10], D. Tzanetatos[10], C. Valieri[17], V. Van Elewyck[4,49], G. Vasileiadis[53], F. Versari[17,18], S. Viola[20], D. Vivolo[6,29], G. de Wasseige[4], J. Wilms[54], R. Wojaczyński[48], E. de Wolf[15,27], T. Yousfi[23], S. Zavatarelli[11], A. Zegarelli[30,8], D. Zito[20], J. D. Zornoza[5], J. Zúñiga[5], N. Zywucka[21].

[1]Aix Marseille Univ, CNRS/IN2P3, CPPM, Marseille, France.
[2]INFN, Sezione di Catania, Via Santa Sofia 64, Catania, 95123 Italy.
[3]Université de Strasbourg, CNRS, IPHC UMR 7178, F-67000 Strasbourg, France.
[4]Université de Paris, CNRS, Astroparticule et Cosmologie, F-75013 Paris, France.
[5]IFIC - Instituto de Física Corpuscular (CSIC - Universitat de València), c/Catedrático José Beltrán, 2, 46980 Paterna, Valencia, Spain.
[6]INFN, Sezione di Napoli, Complesso Universitario di Monte S. Angelo, Via Cintia ed. G, Napoli, 80126 Italy.
[7]Università di Napoli "Federico II", Dip. Scienze Fisiche "E. Pancini", Complesso Universitario di Monte S. Angelo, Via Cintia ed. G, Napoli, 80126 Italy.
[8]INFN, Sezione di Roma, Piazzale Aldo Moro 2, Roma, 00185 Italy.
[9]Universitat Politècnica de Catalunya, Laboratori d'Aplicacions Bioacústiques, Centre Tecnològic de Vilanova i la Geltrú, Avda. Rambla Exposició, s/n, Vilanova i la Geltrú, 08800 Spain.
[10]NCSR Demokritos, Institute of Nuclear and Particle Physics, Ag. Paraskevi Attikis, Athens, 15310 Greece.
[11]INFN, Sezione di Genova, Via Dodecaneso 33, Genova, 16146 Italy.
[12]University of Granada, Dept. of Computer Architecture and Technology/CITIC, 18071 Granada, Spain.
[13]Friedrich-Alexander-Universität Erlangen-Nürnberg, Erlangen Centre for Astroparticle Physics, Erwin-Rommel-Straße 1, 91058 Erlangen, Germany.
[14]Universitat Politècnica de València, Instituto de Investigación para la Gestión Integrada de las Zonas Costeras, C/ Paranimf, 1, Gandia, 46730 Spain.
[15]Nikhef, National Institute for Subatomic Physics, PO Box 41882, Amsterdam, 1009 DB Netherlands.
[16]University Mohammed V in Rabat, Faculty of Sciences, 4 av. Ibn Battouta, B.P. 1014, R.P. 10000 Rabat, Morocco.
[17]INFN, Sezione di Bologna, v.le C. Berti-Pichat, 6/2, Bologna, 40127 Italy.

[1]also at Dipartimento di Fisica, INFN Sezione di Padova and Università di Padova, I-35131, Padova, Italy

[18]Università di Bologna, Dipartimento di Fisica e Astronomia, v.le C. Berti-Pichat, 6/2, Bologna, 40127 Italy.
[19]KVI-CART University of Groningen, Groningen, the Netherlands.
[20]INFN, Laboratori Nazionali del Sud, Via S. Sofia 62, Catania, 95123 Italy.
[21]North-West University, Centre for Space Research, Private Bag X6001, Potchefstroom, 2520 South Africa.
[22]Instituto Español de Oceanografía, Unidad Mixta IEO-UPV, C/ Paranimf, 1, Gandia, 46730 Spain.
[23]University Mohammed I, Faculty of Sciences, BV Mohammed VI, B.P. 717, R.P. 60000 Oujda, Morocco.
[24]Subatech, IMT Atlantique, IN2P3-CNRS, Université de Nantes, 4 rue Alfred Kastler - La Chantrerie, Nantes, BP 20722 44307 France.
[25]Università di Salerno e INFN Gruppo Collegato di Salerno, Dipartimento di Matematica, Via Giovanni Paolo II 132, Fisciano, 84084 Italy.
[26]ISS, Atomistilor 409, Măgurele, RO-077125 Romania.
[27]University of Amsterdam, Institute of Physics/IHEF, PO Box 94216, Amsterdam, 1090 GE Netherlands.
[28]TNO, Technical Sciences, PO Box 155, Delft, 2600 AD Netherlands.
[29]Università degli Studi della Campania "Luigi Vanvitelli", Dipartimento di Matematica e Fisica, viale Lincoln 5, Caserta, 81100 Italy.
[30]Università La Sapienza, Dipartimento di Fisica, Piazzale Aldo Moro 2, Roma, 00185 Italy.
[31]Università di Bologna, Dipartimento di Ingegneria dell'Energia Elettrica e dell'Informazione "Guglielmo Marconi", Via dell'Università 50, Cesena, 47521 Italia.
[32]Cadi Ayyad University, Physics Department, Faculty of Science Semlalia, Av. My Abdellah, P.O.B. 2390, Marrakech, 40000 Morocco.
[33]University of the Witwatersrand, School of Physics, Private Bag 3, Johannesburg, Wits 2050 South Africa.
[34]Università di Catania, Dipartimento di Fisica e Astronomia "Ettore Majorana", Via Santa Sofia 64, Catania, 95123 Italy.
[35]INFN, LNF, Via Enrico Fermi, 40, Frascati, 00044 Italy.
[36]INFN, Sezione di Bari, via Orabona, 4, Bari, 70125 Italy.
[37]International Centre for Radio Astronomy Research, Curtin University, Bentley, WA 6102, Australia.
[38]University of Bari, Via Amendola 173, Bari, 70126 Italy.
[39]University Würzburg, Emil-Fischer-Straße 31, Würzburg, 97074 Germany.
[40]Western Sydney University, School of Computing, Engineering and Mathematics, Locked Bag 1797, Penrith, NSW 2751 Australia.
[41]Università di Salerno e INFN Gruppo Collegato di Salerno, Dipartimento di Fisica, Via Giovanni Paolo II 132, Fisciano, 84084 Italy.
[42]Università di Genova, Via Dodecaneso 33, Genova, 16146 Italy.
[43]Normandie Univ, ENSICAEN, UNICAEN, CNRS/IN2P3, LPC Caen, LPCCAEN, 6 boulevard Maréchal Juin, Caen, 14050 France.
[44]University of Granada, Dpto. de Física Teórica y del Cosmos & C.A.F.P.E., 18071 Granada, Spain.
[45]NIOZ (Royal Netherlands Institute for Sea Research), PO Box 59, Den Burg, Texel, 1790 AB, the Netherlands.
[46]Tbilisi State University, Department of Physics, 3, Chavchavadze Ave., Tbilisi, 0179 Georgia.
[47]Leiden University, Leiden Institute of Physics, PO Box 9504, Leiden, 2300 RA Netherlands.
[48]National Centre for Nuclear Research, 02-093 Warsaw, Poland.
[49]Institut Universitaire de France, 1 rue Descartes, Paris, 75005 France.
[50]University of Johannesburg, Department Physics, PO Box 524, Auckland Park, 2006 South Africa.
[51]Eberhard Karls Universität Tübingen, Institut für Astronomie und Astrophysik, Sand 1, Tübingen, 72076 Germany.
[52]Università di Pisa, Dipartimento di Fisica, Largo Bruno Pontecorvo 3, Pisa, 56127 Italy.
[53]Laboratoire Univers et Particules de Montpellier, Place Eugène Bataillon - CC 72, Montpellier Cédex 05, 34095 France.
[54]Friedrich-Alexander-Universität Erlangen-Nürnberg, Remeis Sternwarte, Sternwartstraße 7, 96049 Bamberg, Germany.
[55]Université de Haute Alsace, 68100 Mulhouse Cedex, France.
[56]University of Münster, Institut für Kernphysik, Wilhelm-Klemm-Str. 9, Münster, 48149 Germany.
[57]Utrecht University, Department of Physics and Astronomy, PO Box 80000, Utrecht, 3508 TA Netherlands.
[58]INFN, CNAF, v.le C. Berti-Pichat, 6/2, Bologna, 40127 Italy.